Underwater ambient noise on the Chukchi Sea continental slope from 2006–2009

Ethan H Roth,[a)] John A. Hildebrand, and Sean M. Wiggins
Scripps Institution of Oceanography, University of California, San Diego, 9500 Gilman Drive, La Jolla, California 92093-0205

Donald Ross
2404 Loring Street, Box 101, San Diego, California 92109

(Received 26 January 2011; revised 18 October 2011; accepted 1 November 2011)

From September 2006 to June 2009, an autonomous acoustic recorder measured ambient noise north of Barrow, Alaska on the continental slope at 235 m depth, between the Chukchi and Beaufort Seas. Mean monthly spectrum levels, selected to exclude impulsive events, show that months with open-water had the highest noise levels (80–83 dB re: 1 μPa^2/Hz at 20–50 Hz), months with ice coverage had lower spectral levels (70 dB at 50 Hz), and months with both ice cover and low wind speeds had the lowest noise levels (65 dB at 50 Hz). During ice covered periods in winter-spring there was significant transient energy between 10 and 100 Hz from ice fracture events. During ice covered periods in late spring there were significantly fewer transient events. Ambient noise increased with wind speed by ~1 dB/m/s for relatively open-water (0%–25% ice cover) and by ~0.5 dB/m/s for nearly complete ice cover (> 75%). In September and early October for all years, mean noise levels were elevated by 2–8 dB due to the presence of seismic surveys in the Chukchi and Beaufort Seas. © *2012 Acoustical Society of America*. [DOI: 10.1121/1.3664096]

PACS number(s): 43.30.Nb, 43.50.Rq 43.60.Cg [RAS] Pages: 104–110

I. INTRODUCTION

Underwater noise in the Arctic Ocean is strongly influenced by sea ice. Low-frequency noise is created by ice deformation along pressure ridges (Macpherson, 1962; Greene and Buck, 1964; Milne and Ganton, 1964; Payne, 1964; Ganton and Milne, 1965). In marginal ice zones, noise results from interaction of wind-driven ocean waves with ice floes (Makris and Dyer, 1986; Makris and Dyer, 1991). Sea ice also plays a role in limiting sound propagation, as scattering occurs along the rough underside of ice boundaries at higher rates than for scattering from the surface of the open sea (Diachok, 1980). Recently, the Arctic Ocean has experienced diminished ice cover as record lows have been measured for sea ice thickness, a proxy for multiyear ice (Stroeve *et al.*, 2007). Perennial pack ice is diminishing while thin seasonal pack ice is more prevalent. These changes in sea ice affect the sound sources, both natural and anthropogenic, which contribute to ambient noise.

During September 2006 to June 2009, we conducted passive acoustic monitoring on the Chukchi Sea continental slope, collecting a nearly continuous record of offshore sound. We report seasonal changes in ambient noise levels correlated with sea ice dynamics, wind speed, and seismic surveys occurring in the Chukchi and Beaufort Seas.

II. BACKGROUND

A. Arctic ambient noise

The mechanisms responsible for Arctic Ocean underwater noise have been elucidated by studies conducted over the past 50 years. The dependency of specific noise source locations in relation to the dynamics of sea ice was studied from ice camps moving with the drifting floe pack, suspending hydrophones a few meters below the ice (Buck and Greene, 1964). An array of drifting buoys deployed in the Beaufort Sea provided one of the most complete records of long-term variability and spatial coherence of low-frequency sound in the Arctic (Lewis and Denner, 1987). A bottom-mounted differential pressure gauge was used to study ultra-low frequency ambient noise, and found that Arctic spectra are far less energetic than those on either Pacific or Atlantic seafloors (Webb and Schultz, 1992). A bottom-mounted hydrophone array was used to document the contribution of Arctic Basin micro-earthquakes to ambient noise (Sohn and Hildebrand, 2001).

Arctic underwater noise is impulsive, and its temporal distribution can be highly non-Gaussian due to sea ice dynamics. For shore-fast winter and spring pack ice, tensile cracks at the surface caused by decreasing air temperatures act like point-sources of noise. Factures are initiated by large-scale forces such as wind, current, or sustained cooling with the passage of a cold front (Zakarauskas *et al.*, 1991; Lewis, 1994). Likewise, local meteorological conditions such as wind speed, snow cover, or ice fog can act on the ice surface to couple sound underwater, producing high-frequency (>1 kHz) noise (Ganton and Milne, 1965; Lewis and Denner, 1988b).

Diverse mechanisms contribute to Arctic ambient noise variability. During summer and fall, the relative motion and deformation of ice floes moving through surface waters create low-frequency (<1 kHz) noise (Milne and Ganton, 1964). Likewise, the differential motions of floes during ice formation lead to noise from convergence and pressure

a)Author to whom correspondence should be addressed. Electronic mail: rothethan@gmail.com

ridging (Lewis and Denner, 1988a). Exceptionally low noise levels can occur under ice-covered conditions, owing to the suppression of breaking waves and other near-surface noise mechanisms. However, during periods of ice cover noise levels may increase due to ice dynamics, particularly in winter when noise levels are typically equivalent to that of sea state three open-water conditions (Milne and Ganton, 1964; Payne, 1964). Noise directionality is highly anisotropic during quiet periods, while during noisy periods it is nearly isotropic due to sea ice dynamics (Diachok, 1980). Under high noise conditions, most sound comes from nearby sources (<1 km), while under median or lower noise conditions, the sound dominantly comes from more distant sources (9–100 km), especially for frequencies between 10 and 50 Hz (Buck and Wilson, 1986).

B. Arctic sound propagation

Ray paths near the sea surface in the Arctic Ocean are refracted upward, and repeatedly reflect off the sea surface or scatter off the rough underside of sea ice (Diachok, 1980), resulting in substantial long-range transmission loss (LePage and Schmidt, 1994). The reflection of sound off the underside of the ice makes sound propagation in the Arctic highly dependent on sea ice conditions. Backscatter measurements show that pressure ridges are primarily responsible for the scattering of sound at high frequencies (>10 kHz) (Berkson *et al*., 1973). Reflection loss off smooth, flat ice accounts for much of the transmission loss between 200 Hz and 1 kHz, since smooth ice comprises most of the Arctic ice cover (Yang and Votaw, 1981).

Sound attenuation through repeated under-ice reflections is frequency dependent. As frequency increases, so does reflection loss and scattering. The loss is dependent upon the height and correlation length of ice roughness, as well as the ice thickness (Diachok and Winokur, 1974; Diachok, 1976; Gavrilov and Mikhalevsky, 2006). High frequency sound cannot travel long distances, and at frequencies >1 kHz sounds are usually produced locally. On the other hand, very low frequency sounds (<35 Hz) contribute at much farther distances since their wavelengths are not subject to under-ice attenuation (Milne and Ganton, 1964). Studies in the Arctic have also shown that at ranges up to 50 km, bottom-reflected rays are a major part of the total received energy (Buck and Greene, 1964). In shallow water, where the acoustic wavelengths are comparable to the ocean depth, transmission loss from bottom interaction can be significant (Diachok, 1976).

III. METHODS

A. Acoustic measurements

From September 2006 to June 2009, a High-frequency Acoustic Recording Package (HARP) (Wiggins and Hildebrand, 2007) was deployed north of Barrow, Alaska (72° 27.7′N, 157° 24.0′W) on the continental slope at 235 m depth between the shallow Chukchi Sea and deep Beaufort Sea (Fig. 1). The HARP recorded continuously (2006–2007) or with a 50% duty cycle (2007–2009) at a

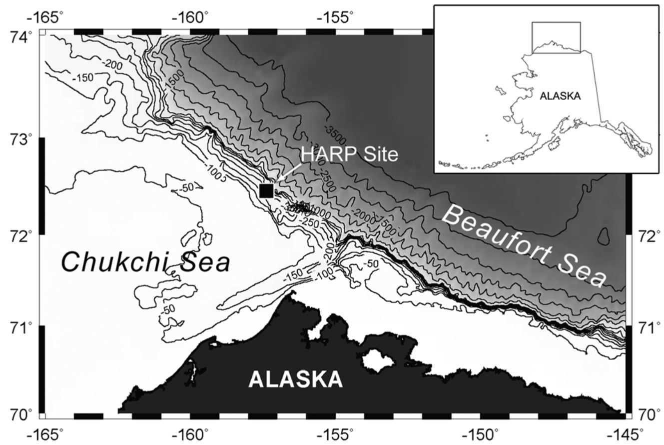

FIG. 1. Location of the HARP site (72° 27.5′ N, 157° 23.4′ W, 235 m depth) along the continental slope, north of Barrow, Alaska. The study site is near the border between the Chukchi and Beaufort Seas. Bathymetric contours are in meters.

32 kHz sample rate, using a 16-bit data-logging system with a total storage capacity of almost 2 Terabytes. Each summer during open-water conditions, the HARP data were retrieved, and the instrument was redeployed with new hard disks and batteries. Hydrophone calibrations were conducted at the Scripps Institution of Oceanography and at the U.S. Navy's Transducer Evaluation Center (TRANSDEC) in San Diego, California. The TRANSDEC calibration verified the expected hydrophone response based on preamplifier measurements and the manufacturer-specified sensitivity of the transducers to be within ±1–2 dB of the measured response.

Spectrum measurements (reported as root-mean-square re: 1 μPa^2/Hz) were produced using 200 s samples of continuous data with no overlap between each spectral average using the *Goertzel* algorithm to calculate power spectral densities from discrete-time Fast-Fourier Transforms (FFT). All spectra were processed with a *Hanning* window and 32 000-point FFT length, yielding 1 Hz frequency bins. Average power spectral densities (PSD) over the 10–250 Hz frequency band were computed both including and excluding transient signals and acoustic events. Basic statistics were computed from the probability distribution of these samples. Two frequencies (50 and 500 Hz) were chosen to illustrate cumulative distribution functions. Spectral averaging statistics were performed on a logarithmic scale. Skewness and kurtosis were calculated from the probability distributions. Skewness, a measure of asymmetry, is the third standardized moment, defined as μ_3/σ^3, where μ_3 is the third moment about the mean, and σ is the standard deviation. Kurtosis, a measure of peakedness, is the fourth standardized moment, defined as μ_4/σ^4. Subtracting 3 yields excess Kurtosis, corrected so that it is zero for a normal distribution.

The dependence of ambient noise on wind was tested for two different surface conditions: 0%–25% and 75%–100% ice cover. Two-day averaged sound spectrum levels at 250 Hz were plotted as a function of mean wind speed, and log transforms were fitted to each set of data. The variances were compared, and correlation coefficients

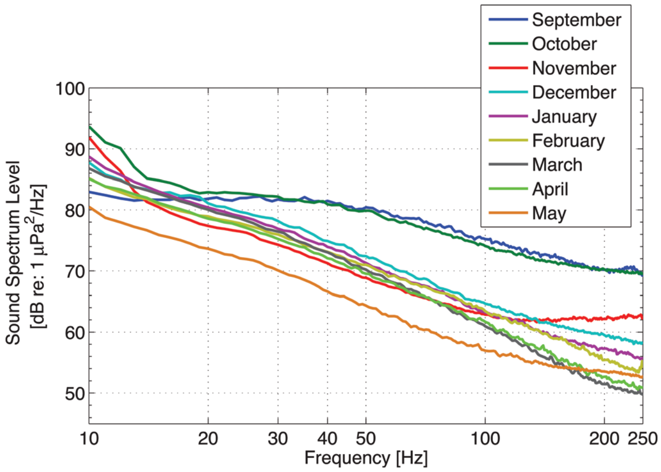

FIG. 2. Mean monthly sound spectum levels from September 2006 to May 2007. Each monthly average is based on 200-s samples, selected when no transient signals are present.

calculated by finding the zeroth lag of the normalized covariance function.

To estimate the noise contribution of seismic surveys during the open water seasons in 2006, 2007, and 2008, the data were manually categorized as having nearby (strong), distant (weak) or no airgun shot arrivals. For each season, sound spectrum levels were averaged separately for strong, weak, or no airgun presence, allowing comparison.

B. Sea ice measurements

Sea ice concentration was estimated from satellite measurements of backscattered microwave radiation. Approximately 6 km by 4 km spatial resolution is available using the Special Sensor Microwave/Imager (SSM/I) at 89 GHz and the ARTIST Sea Ice (ASI) algorithm (Spreen *et al.*, 2008). Gridded daily mean sea ice concentrations were extracted for the region 68°–76° N and 180°–130° W. Time-series analysis was performed using Windows Image Manager (WIM) and WIM Automation Module (WAM) software (Kahru, 2000). The 6 km pixels in polar stereographic projection were remapped to a 4 km pixel linear projection. A circular mask with a 100 nm radius, centered on the instrument site, was used to match the sound propagation range appropriate for low frequency noise. WAM computed the percentage ice coverage arithmetic mean, variance, and median for each day. On days when no valid data appeared in the mask area due to a spatial gap in satellite passes, linear interpolation between adjacent days was applied.

C. Wind measurements

Daily values for peak wind speed, average wind speed, and peak wind direction were obtained from the U.S. National Weather Service at http://www.arh.noaa.gov/clim/akcoopclim.php (date last viewed 6/1/10). Measurements were made at Barrow, Alaska (71° 17.12′ N, 156° 45.95′ W), approximately 130 km south of the instrument site, by an automated surface observing system 10 m above sea level.

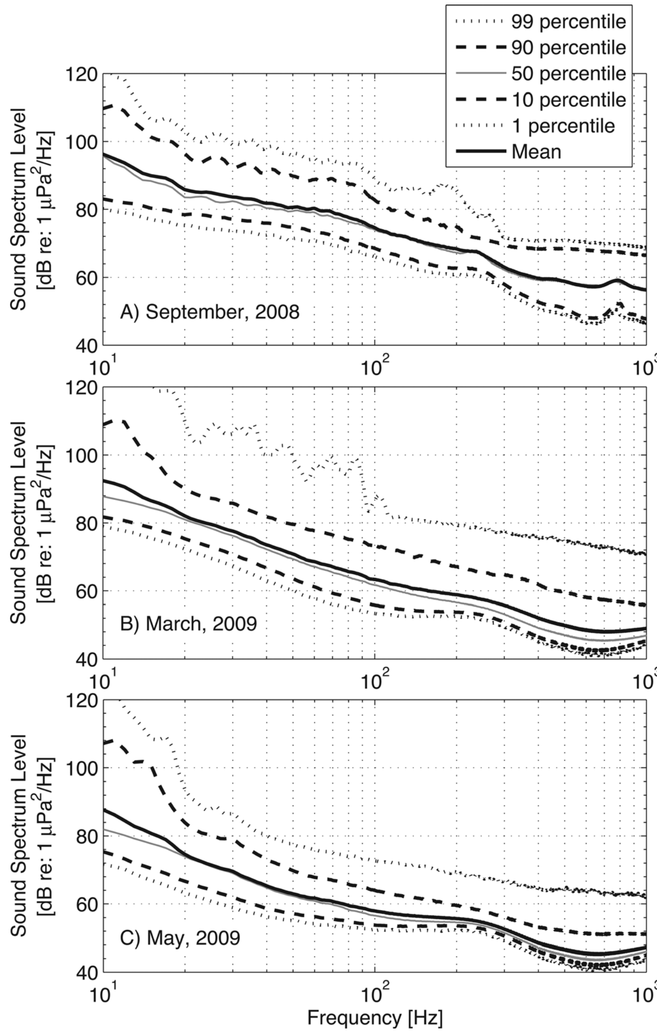

FIG. 3. Sound spectrum levels for the months of (a) September 2008, (b) March 2009, and (c) May 2009. Distributions are represented by the mean, 99th, 90th, 50th (median), 10th, and 1st percentiles. Distributions are long-tailed for higher values, with mean values greater than the median.

IV. RESULTS

A. Background noise levels: Excluding impulsive events

Mean monthly sound spectrum levels, selected to exclude impulsive events, are presented in Fig. 2. September and October, the months with little or no ice coverage, had the highest noise, reaching their maximum spectrum levels (80–83 dB re: 1μPa^2/Hz) at 20–50 Hz, and decreasing at $\sim$5 dB/octave above 50 Hz. All other months have lower noise levels, (e.g. 70 dB at 50 Hz) and decrease at $\sim$8 dB/octave. May, a month with both ice cover and low wind speeds, had the lowest noise levels (65 dB at 50 Hz). Months with ice cover had similar noise levels in the band 15–150 Hz, but diverged above 150 Hz.

B. Noise levels including impulsive events

Sound spectrum levels that include impulsive events are shown for selected months in Fig. 3. Three months were chosen to compare periods with open-water conditions

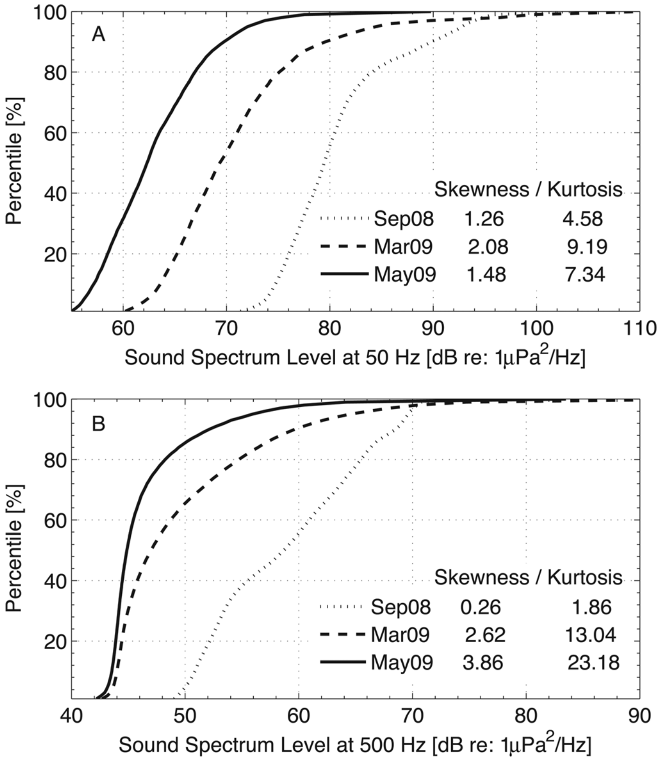

FIG. 4. Sound spectrum level cumulative distribution functions for the months of September 2008, March 2009, and May 2009 at (a) 50 Hz and (b) 500 Hz. The skewness and excess kurtosis are calculated for each month (inset).

(September 2008), ice coverage with transient events (March 2009), and ice coverage without transient events (May 2009).

During open-water conditions (September 2008), ambient noise levels were higher on average and the curves have the smallest frequency dependence [Fig. 3(a)]. Transient energy is apparent in the 90th and 99th percentile curves, particularly for frequencies < 100 Hz. For ice coverage in winter-spring (March 2009), mean noise levels are 5–10 dB lower than for open-water conditions. However, there also was significant transient energy between 10 and 100 Hz, apparent in the 99th percentile curve [Fig. 3(a)]. For ice coverage in late spring (May 2009), average noise levels were remarkably low, as much as 20 dB below open water conditions [Fig. 3(c)], with little or no suggestion of transient events in the 90th or 99th percentile curves.

Cumulative distribution functions (CDFs) at 50 and 500 Hz are shown in Fig. 4 for the same months shown in Fig. 3. All three months exhibit a positive skew, being long-tailed for high noise levels. The skewness is lowest for September (open water) and increases during March/May (ice cover), particularly at 500 Hz. Excess kurtosis also increases between September and March/May, and the difference is again more pronounced at 500 Hz. Higher skewness and kurtosis suggests that much of the variance is the result of irregular impulses of noise.

C. Environmental correlates

Daily-mean sound spectrum levels at 100 Hz are plotted along with average wind speed and mean sea ice cover in Fig. 5. Several events have been highlighted where strong correlation exists between the three datasets (gray bars in Fig. 5). In October 2006, a large storm generated the highest average wind speeds seen in the absence of extensive ice cover (<50%). With a several day lag, ambient noise levels increased and stayed correlated with wind speed throughout October, until ice formation increased. A storm in February 2007 produced winds strong enough to increase pressure ridging and break up the consolidated pack ice, creating temporary leads or small pockets of open water (∼10%). Shortly thereafter, sound spectrum levels increased dramatically until there was a return to full ice coverage. Ice formation in November 2007 triggered two of the highest peaks in ambient noise levels, which were followed by a brief period in the beginning of December when there was a substantial loss of sea ice (∼25%). Starting in mid-April 2008, the ice coverage fluctuated in response to two wind events that lasted until mid-May. Although the lag time is not clear, noise levels increased sharply for several days before the winds subsided. During ice formation in 2008, strong winds again

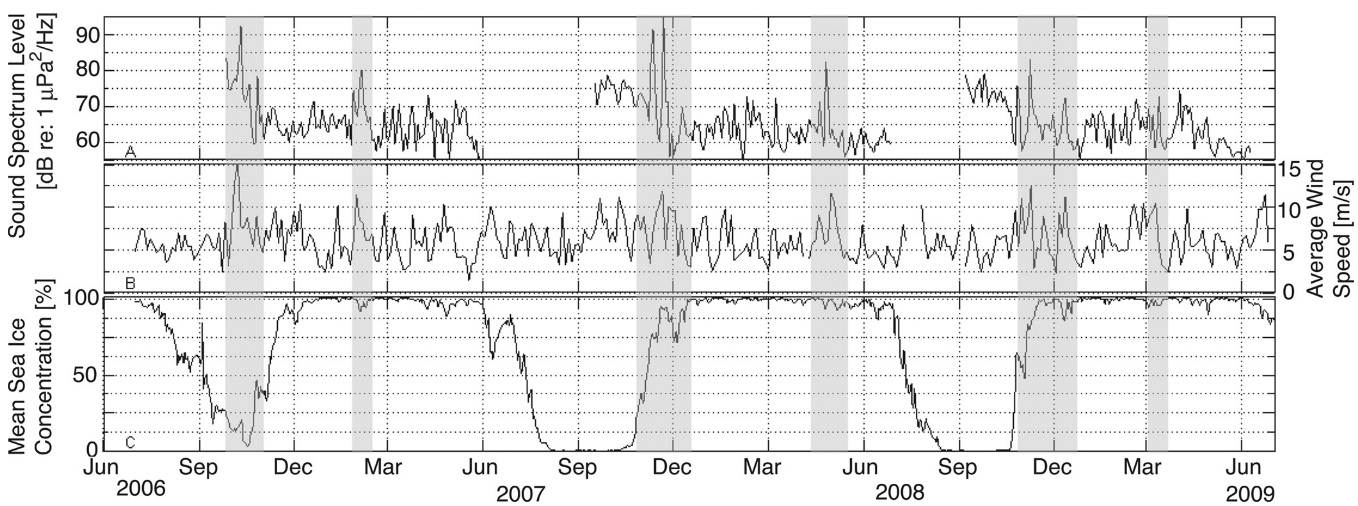

FIG. 5. (a) Time series of mean sound-pressure spectrum levels at 100 Hz, (b) three-day averaged wind speed values from the weather station in Barrow, Alaska, and (c) the percentage of sea ice cover from AMSR-E for a 100 nm radius centered on the instrument site. Shaded periods of time show correlations between significant ambient noise and weather events.

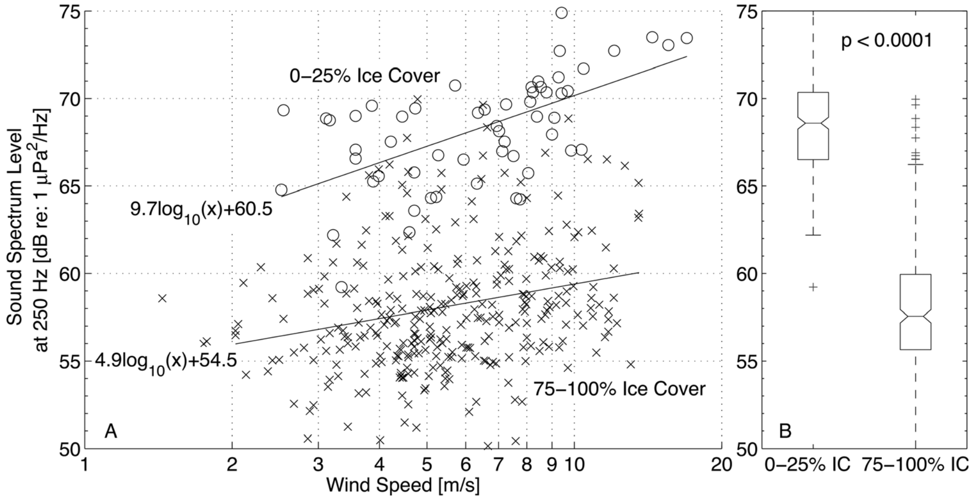

FIG. 6. (a) Two-day averaged sound spectrum levels at 250 Hz versus mean wind speed from September 2006 to June 2009. The "[circo]" represents sound spectrum levels during 0%–25% ice cover (IC), while the "x" represents sound spectrum levels during 75%–100% ice cover. Log transforms are fitted to each data set to estimate the dependence of ambient noise on wind. (b) An analysis of variance for the two surface conditions shows that the two groups of data are distinct from one another and the resulting *p*-value is small.

gave rise to high spectrum levels in early November, but no correlation appears to exist in late November when the mean ice coverage was nearly 100%. In December, high wind speed reduced ice coverage in the area by as much as 15%, generating a peak in ambient noise levels. In March of 2009, when the Arctic reached its maximum sea ice extent, storm-generated winds reduced ice coverage slightly, and noise levels showed impulsive peaks in the time series.

The dependence of ambient noise on wind speed (Ross, 1976) was tested from September 2006 to June 2009 for two different surface conditions: relatively open-water (0%–25% ice cover) and nearly full ice cover (>75%). Two-day averaged sound spectrum levels at 250 Hz are plotted as a function of mean wind speed on a logarithmic scale [Fig. 6(a)]. The two surface conditions produce different relationships between noise and wind speed. Sound spectrum levels with 0%–25% ice cover are consistently higher by about 8–12 dB than with 75%–100% ice cover. Furthermore, open-water conditions exhibit a steeper slope ($\sim$1 dB/m/s) for increasing wind speed compared to ice-covered conditions ($\sim$0.5 dB/m/s), for wind speeds of 3–10 m/s.

The correlation coefficient between ambient noise and wind speed is higher for 0%–25% ice cover (0.62), and than it is for 75%–100% ice cover (0.28). This suggests that wind speed is a better predictor for noise during open-water conditions, than during ice-covered conditions. Based on Fig. 5, there appears to be a variable lag time between wind speed and noise levels when ice coverage is greater than 75%. This lag time is likely a function of ice and snow thickness (Diachok, 1976; Gavrilov and Mikhalevsky, 2006). An analysis of variance [Fig. 6(b)] suggests a significant difference between the sound spectrum levels for the two surface conditions ($p \ll 0.0001$).

D. Anthropogenic noise

In September and early October for all three years, noise levels were elevated due to the presence of seismic surveys in the Chukchi and Beaufort Seas. Manual scans of the sound data revealed that airguns were detectable half or more of the time (Table I), making a significant contribution to the noise field. Figure 7 shows a long-term spectral plot for the period when airguns were observed between 16 September to 7 October, 2007. A total of 31 bouts of airguns were detected spanning 511 hourly windows, versus 79 hourly windows with no detectable airguns. The airgun signatures varied in intensity, presumably owing to the distance to the airgun source. The frequency structure of the airgun arrivals

TABLE I. Airgun surveys detected and permitted/reported during 2006–2008 in the Chukchi and Beaufort Seas.

Year	Received level	Number bouts	Start date	End date	Hours	%Total hours	Seismic surveys permitted[a]	Trackline distance (km)[a]
2006	Strong	11	9/26	10/4	97	48		
	Weak	2	9/26	9/26	2	1		
	None				103	51		
	Total				201		3	24455
2007	Strong	17	9/18	10/7	267	52		
	Weak	14	9/16	10/4	165	32		
	None				79	16		
	Total				511		3	8576
2008	Strong	30	9/6	10/1	358	59		
	Weak	21	9/6	10/1	208	34		
	None				41	7		
	Total				607		5	20824

[a]From http://www.nmfs.noaa.gov/pr/permits/incidental.htm (Last viewed 1/18/11) http://alaska.boemre.gov/re/recentgg/RECENTGG.HTM (Last viewed 1/18/11) and Hutchinson *et al.* (2009)

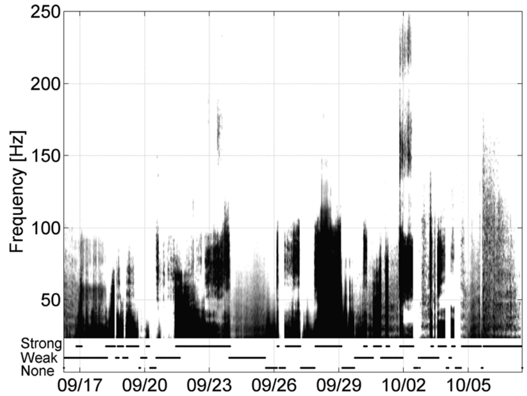

FIG. 7. Long-term spectrogram of noise during 16 September to 7 October 2007. Airgun bouts appear with sharp temporal boundaries. Lower bars show timeline of airgun categorization by manual inspection of the time-series data as strong, weak, or none—periods without airguns.

also varied, sometimes showing peaks and troughs of energy across the 10–220 Hz band.

The airgun contribution to ambient noise levels is quantified in Fig. 8, by plotting the average sound spectral level for the time period displayed in Fig. 7. Periods of strong airgun presence (52% of time) have spectral levels elevated by 3–8 dB, and periods of weak airgun presence (32% of time) are elevated by 2–5 dB, relative to periods with no airgun presence (16% of time).

Due to modal dispersion from multipath propagation in shallow water, the originally impulsive airgun signals may arrive at the instrument with increased time-spread (Medwin, 2005). The spectrogram in Fig. 9 shows two airgun shots, each containing four modes observed as frequency upsweeps. The modes are spread-out over about 5 s and most of the energy is between 7 and 80 Hz.

V. DISCUSSION

During the summer and fall, open-water conditions lead to high levels of ambient noise (Fig. 2). September represents the open-water season and has average noise levels that are 5–20 dB higher than seasons with ice cover (Figs. 3 and 4). In the absence of shipping or airguns, wind-driven surface waves are the dominate noise source during open-

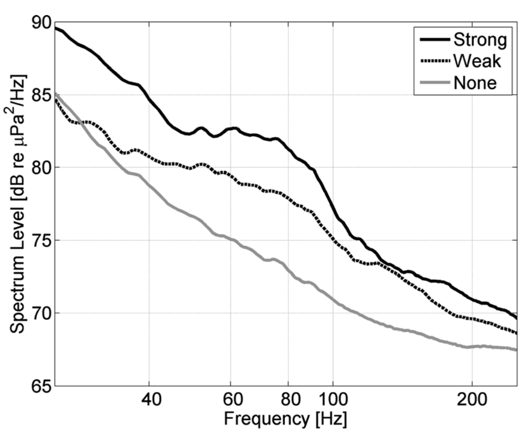

FIG. 8. Sound spectrum levels for the periods of airgun usage shown in Fig. 7, categorized as either strong, weak, or none.

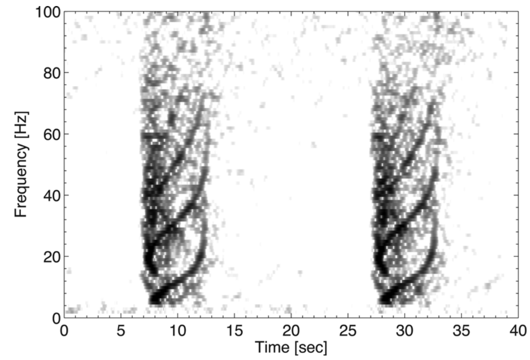

FIG. 9. Modal dispersion of two airgun shots, received by the hydrophone at 10 m above the seafloor. The shots—20 s apart—each contain four modes observed as frequency upsweeps. The modes are spread-out over more than 5 s with energy between 7 and 80 Hz.

water conditions. Anthropogenic activity contributes to the noise spectrum distributions during summer and fall, as energy is added by seismic surveys and other anthropogenic sources (Figs. 7 and 8). From 10 to 100 Hz these sources dominate the spectra more than half of the time.

Using publicly available documents, such as reports and permit applications, we assessed the extent of seismic survey activity permitted in the vicinity of our study area, the Alaskan Chukchi and Beaufort Seas (Table I). These reports suggest three to five major seismic surveys were conducted each year of our study (2006–2008), using airgun arrays volumes of about 7 000–10 000 in.[3] Although the reports/permits suggest a lower level of activity during the 2007 season (8576 km trackline) than in 2006 or 2008 (24 455 and 20 824 km), we do not see this reflected in the noise data, that suggest an increasing level of airgun activity each successive year of our study (Table I). While the permitted surveys were carried out in and around U.S. waters, there may be additional seismic surveys outside the permitting process that occurred in the adjacent Canadian Beaufort and Russian Arctic, potentially affecting the ambient noise in the Chukchi Sea.

During winter and spring, sea ice strongly influences ambient noise. Lossy sound transmission in ice-covered waters produces noise levels that are low, especially at higher frequencies (Fig. 2). During periods of ice cover, ambient noise includes discrete and impulsive sea ice deformation and fracturing events, which are caused by thermal, wind, drift, and current stresses acting on pack ice. The highest noise levels from these events are seen below 100 Hz [Fig. 3(b)]. These episodes create an overall probability distribution that is both long-tailed and non-stationary (Zakarauskas *et al.*, 1991). In late spring, the ice cover results in exceptionally low ambient noise [Fig. 3(c)]. This is the period when sea ice coverage is high, yet wind speeds are low. The lower spectral levels for months with ice-coverage are often close to median levels, making the distribution short-tailed for lower values.

With this study, we show fluctuations in ambient noise over long periods. Longer time series allow event-based correlations over longer periods. During summer and fall open-water conditions, the peaks and troughs of sound-pressure levels correlate well with those of wind speed

(Figs. 5 and 6). Although more complex, we find that transient weather events also generate high noise levels during periods of full ice cover. When ice coverage is 100%, but ice dynamics have slowed and wind speed is low, ambient noise reaches some of the lowest levels found in the polar ocean.

The Arctic Ocean presents a unique opportunity to observe the dependency of ambient noise on wind in the absence of shipping noise during both open-water and ice-covered conditions. We find that differences in surface conditions result in distinct regimes of ambient noise (Fig. 6). The correlation between wind speed and sound spectrum levels at 250 Hz during 0%–25% ice cover suggests an average increase of about 1 dB/m/s for open-water conditions. The relation between noise and wind speed during 75%–100% ice cover is more complex [Fig. 6(a)] but suggests about 0.5 dB/m/s.

VI. CONCLUSIONS

From 2006–2009, an autonomous acoustic recorder on the Chukchi Sea continental slope monitored underwater sound to characterize temporal and spectral variations of ambient noise. In the absence of transient events, the open-water season had mean noise spectrum levels that were 3–10 dB higher than during the season of ice cover. During periods of ice cover, transient events occur primarily during the winter and early spring, and less so during the late spring. Airgun sounds are present in a substantial portion of the open-water period in the summer and fall, raising average noise levels by 2–8 dB on the continental slope of the Chukchi Sea.

ACKNOWLEDGMENTS

The authors thank Bob Small of the Alaska Department of Fish and Game for providing funding and support through a Coastal Impact Assistance Program (CIAP) grant from MMS. We also thank Robert Suydam and Craig George of the North Slope Borough who provided additional funding and support for data analysis; Caryn Rea of ConocoPhillips and the crew of the M/V Torsvik who provided field and logistical support for the 2006 HARP deployments; Larry Mayer of the University of New Hampshire and the crew of the USCGC Healy who provided field and logistical support for the 2007, 2008, and 2009 HARP retrievals and redeployments; and the Barrow Arctic Science Consortium who provided logistical support. Thanks to all our colleagues in the Scripps Whale Acoustics Lab who assisted with various aspects of this work. This work is dedicated to the Iñupiaq people of Alaska's North Slope for their incredible resilience.

Berkson, J. M., Clay, C. S., and Kan, T. K. (**1973**). "Mapping the underside of arctic sea ice by backscattered sound," J. Acoust. Soc. Am. **53**(3), 777–781.

Buck, B. M., and Greene, C. R. (**1964**). "Arctic deep-water propagation measurements," J. Acoust. Soc. Am. **36**(8), 1526–1533.

Buck, B. M., and Wilson, J. H. (**1986**). "Nearfield noise measurements from an Arctic pressure ridge," J. Acoust. Soc. Am. **80**(1), 256–264.

Diachok, O. (**1980**). "Arctic hydroacoustics," Cold Reg. Sci. Technol. **2**, 186–1201.

Diachok, O. I. (**1976**). "Effects of sea-ice ridges on sound propagation in the Arctic Ocean," J. Acoust. Soc. Am. **59**(5), 1110–1120.

Diachok, O. I., and Winokur, R. S. (**1974**). "Spatial variability of underwater ambient noise at the Arctic ice-water boundary," J. Acoust. Soc. Am. **55**(4), 750–753.

Ganton, J. H., and Milne, A. R. (**1965**). "Temperature- and wind-dependent ambient noise under midwinter pack ice," J. Acoust. Soc. Am. **38**(3), 406–411.

Gavrilov, A. N., and Mikhalevsky, P. N. (**2006**). "Low-frequency acoustic propagation loss in the Arctic Ocean: Results of the Arctic climate observations using underwater sound experiment," J. Acoust. Soc. Am. **119**(6), 3694–3706.

Greene, C. R., and Buck, B. M. (**1964**). "Arctic ocean ambient noise," J. Acoust. Soc. Am. **36**(6), 1218–1220.

Hutchinson, D. R., Jackson, H. R., Shimeld, J. W., Chapman, C. B., Childs, J. R., Funck, T., and Rowland, R. W. (**2009**). "Acquiring marine data in the Canada Basin, Arctic Ocean," Eos Trans. AGU **90**, 197–198.

Kahru, M. (**2000**). "Windows Image Manager-Image display and analysis program for Microsoft Windows with special features for satellite images," from http://wimsoft.com (Last viewed April 6, 2010).

LePage, K., and Schmidt, H. (**1994**). "Modeling of low-frequency transmission loss in the central Arctic," J. Acoust. Soc. Am. **96**(3), 1783–1795.

Lewis, J. K. (**1994**). "Relating Arctic ambient noise to thermally induced fracturing of the ice pack," J. Acoust. Soc. Am. **95**(3), 1378–1385.

Lewis, J. K., and Denner, W. W. (**1987**). "Arctic ambient noise in the Beaufort Sea: Seasonal space and time scales," J. Acoust. Soc. Am. **82**(3), 988–997.

Lewis, J. K., and Denner, W. W. (**1988a**). "Arctic ambient noise in the Beaufort Sea: Seasonal relationships to sea ice kinematics," J. Acoust. Soc. Am. **83**(2), 549–565.

Lewis, J. K., and Denner, W. W. (**1988b**). "Higher frequency ambient noise in the Arctic Ocean," J. Acoust. Soc. Am. **84**(4), 1444–1455.

Macpherson, J. D. (**1962**). "Some under-ice acoustic ambient noise measurements," J. Acoust. Soc. Am. **34**(8), 1149–1150.

Makris, N. C., and Dyer, I. (**1986**). "Environmental correlates of pack ice noise," J. Acoust. Soc. Am. **79**(5), 1434–1440.

Makris, N. C., and Dyer, I. (**1991**). "Environmental correlates of Arctic ice-edge noise," J. Acoust. Soc. Am. **90**(6), 3288–3298.

Medwin, H. (**2005**). *Sounds in the Sea: From Ocean Acoustics to Acoustical Oceanography* (Cambridge University Press, New York), pp. 239–240.

Milne, A. R., and Ganton, J. H. (**1964**). "Ambient noise under Arctic-sea ice," J. Acoust. Soc. Am. **36**(5), 855–863.

Payne, F. A. (**1964**). "Effect of ice cover on shallow-water ambient sea noise," J. Acoust. Soc. Am. **36**(10), 1943–1947.

Ross, D. (**1976**). *Mechanics of Underwater Noise* (Pergamon Press, New York), p. 375.

Sohn, R. A., and Hildebrand, J. A. (**2001**). "Hydroacoustic earthquake detection in the Arctic Basin with the Spinnaker array," Bull. Seismol. Soc. Am. **91**(3), 572–579.

Spreen, G., Kaleschke, L., and Heygster, G. (**2008**). "AMSR-E ASI 6.25 km sea ice concentration data, V5.2," from http://www.iup.physik.uni-bremen.de (Last viewed April 2, 2010).

Stroeve, J., Holland, M. M., Meier, W., Scambos, T., and Serreze, M. (**2007**). "Arctic sea ice decline: Faster than forecast," Geophys. Res. Lett. **34**(9), L09501, doi:10.1029/2007GL029703.

Webb, S. C., and Schultz, A. (**1992**). "Very low frequency ambient noise at the seafloor under the Beaufort Sea icecap," J. Acoust. Soc. Am. **91**(3), 1429–1439.

Wiggins, S. M., and Hildebrand, J. A. (**2007**). "High-frequency Acoustic Recording Package (HARP) for broad-band, long-term marine mammal monitoring," in *International Symposium on Underwater Technology 2007 and International Workshop on Scientific Use of Submarine Cables and Related Technologies 2007* (IEEE, Tokyo, Japan), pp. 551–557.

Yang, T. C., and Votaw, C. W. (**1981**). "Under ice reflectivities at frequencies below 1 kHz," J. Acoust. Soc. Am. **70**(3), 841–851.

Zakarauskas, P., Parfitt, C. J., and Thorleifson, J. M. (**1991**). "Automatic extraction of spring-time Arctic ambient noise transients," J. Acoust. Soc. Am. **90**(1), 470–474.